

Investigation into the excess infrared emission detected from the west hot spot of the radio galaxy Pictor A: a possible evidence of the turbulence acceleration



N. Isobe (ISAS/JAXA; IR)

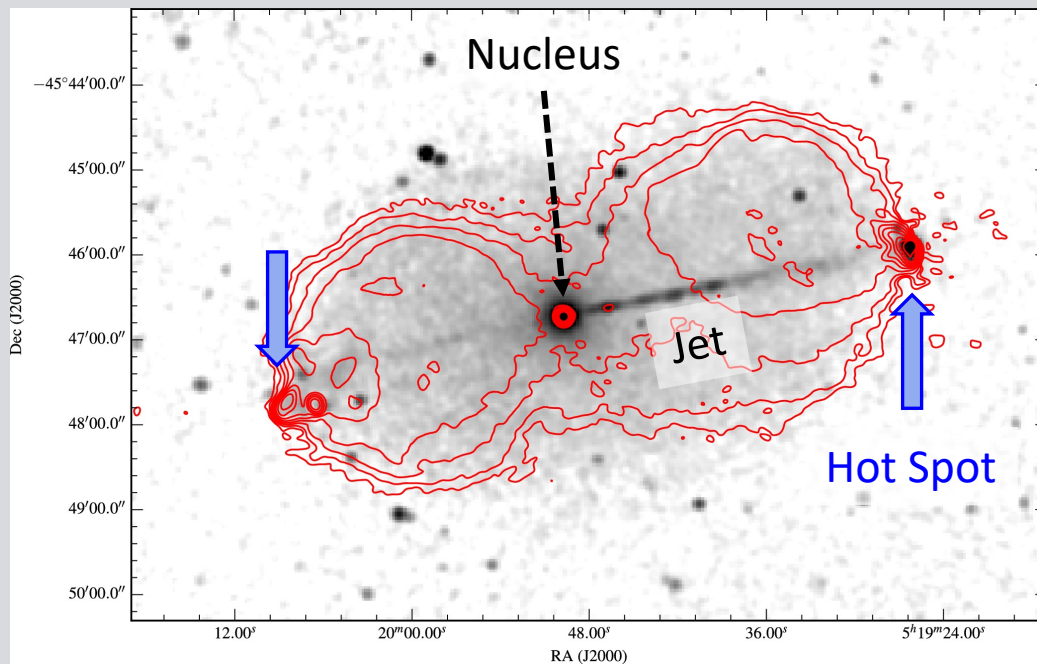
H. Nagai (NAOJ; Radio), M. Kino (Kogakuin University; Radio/Theory)

S. Baba (Kagoshima University; IR), T. Nakagawa (ISAS/JAXA; IR)

Y. Sunada, M. Tashiro (Saitama University; X-ray)

Hot spots of radio galaxies

➤ The radio galaxy Pictor A

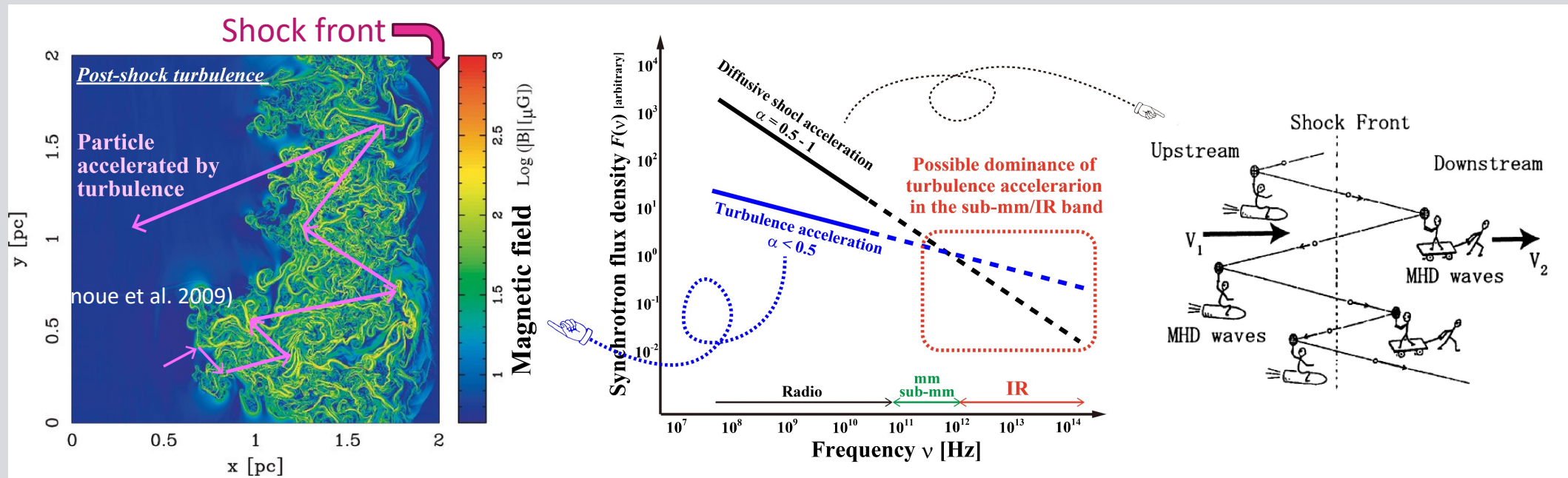


(Radio/X-ray; Hardcastle et al. 2016)

- ✓ Compact regions with a high radio/X-ray flux at the end of the AGN jets
- ✓ Strong **jet-terminal shocks**
 - ✓ Final destination of accretion process
- ✓ **Non-thermal emission** from relativistic electrons
 - ✓ **Synchrotron radio** emission
 - ✓ **Inverse-Compton X-ray** emission
 - ✓ Typical spectral index $\alpha = 0.5 - 1$
 - ✓ Flux density $F_\nu \propto \nu^{-\alpha}$
- ✓ One of the most promising candidates for ultra-high energy cosmic rays
 - ✓ $E > 10^{18}$ eV (Hillas 1984, Kotera & Olinto, 2011)

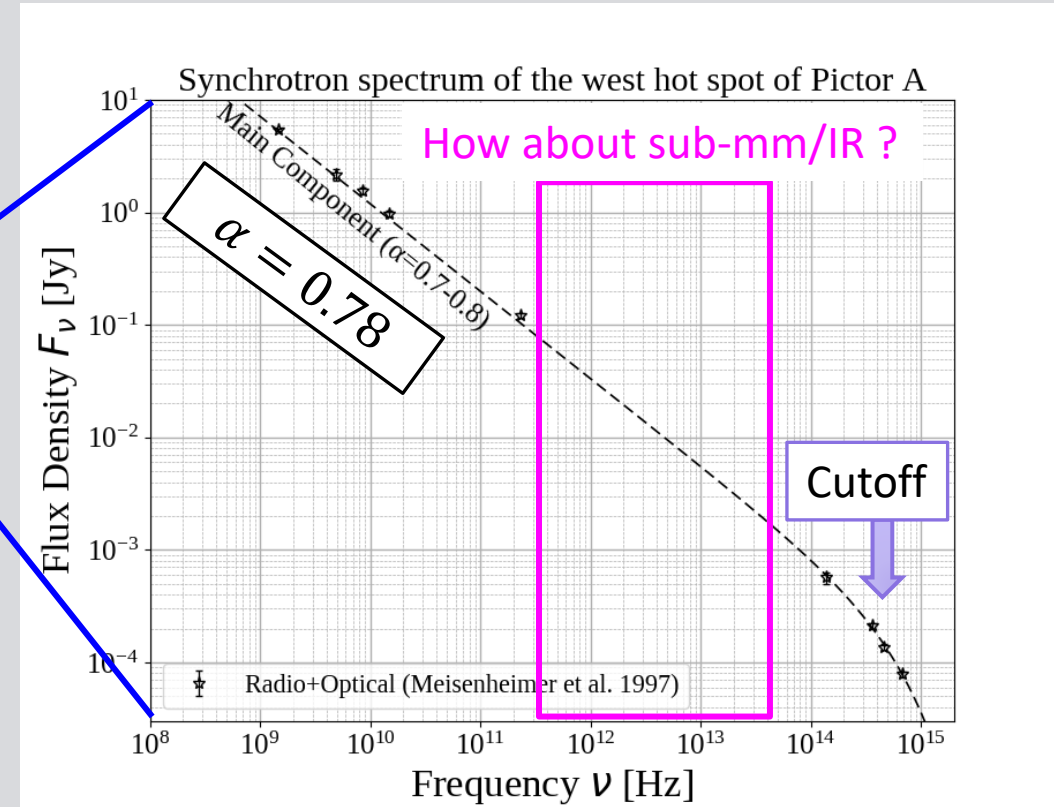
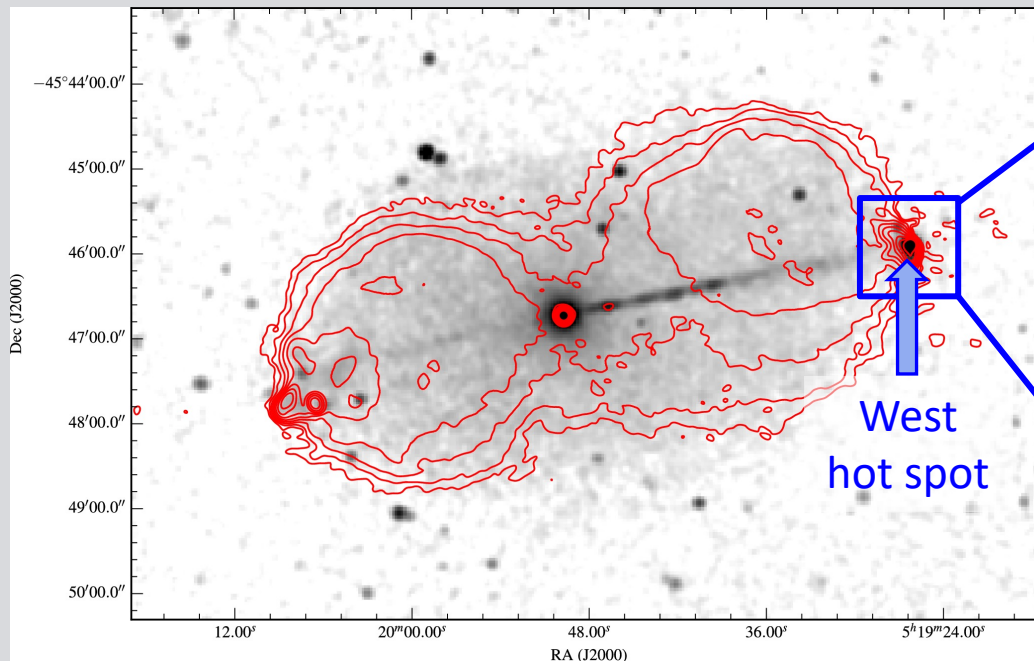
Particle acceleration in the hot spots

- **Turbulence acceleration**
(Fermi-II/stochastic acceleration)
 - **Hard spectrum: $\alpha < 0.5$**
 - No observational evidence
- Relative dominance on the synchrotron spectrum
 - Possible signature of the **turbulence acceleration** in the **sub-mm/IR range**.
- Diffusive shock acceleration
 - Standard picture
 - Spectrum : **$\alpha > 0.5$**



The west hot spot of Pictor A

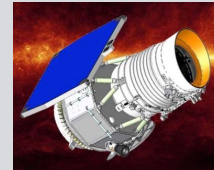
➤ The radio galaxy Pictor A



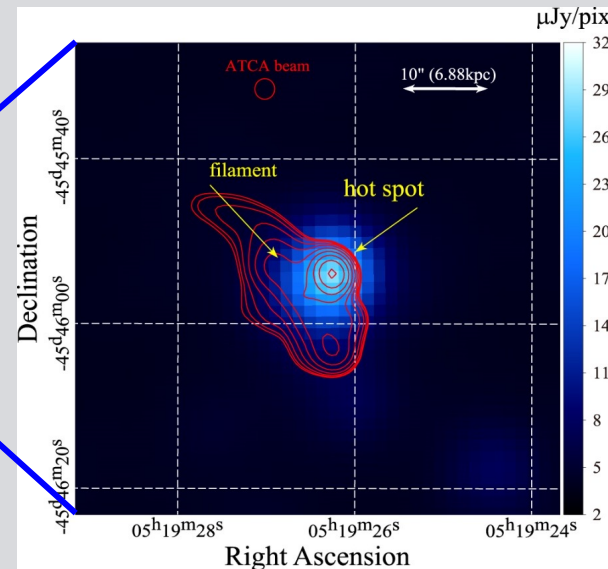
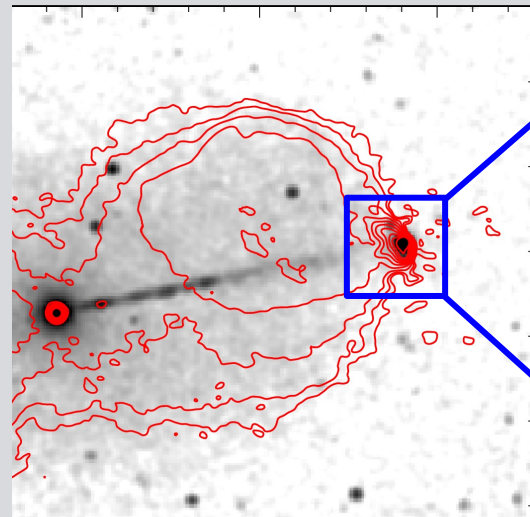
Radio and optical data alone appears to be consistent to the standard diffusive shock acceleration

Infrared search for the turbulence acceleration

- Mid-IR data with WISE (3.4 μm)

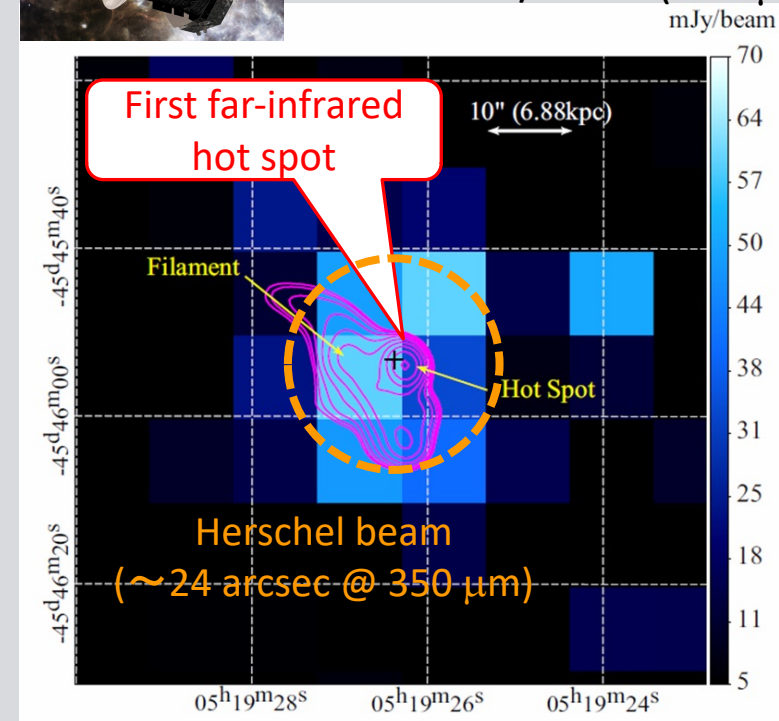
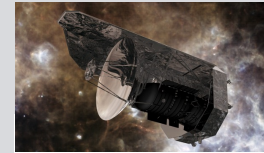


The west hot spot of Pictor A



(Isobe et al. 2017)

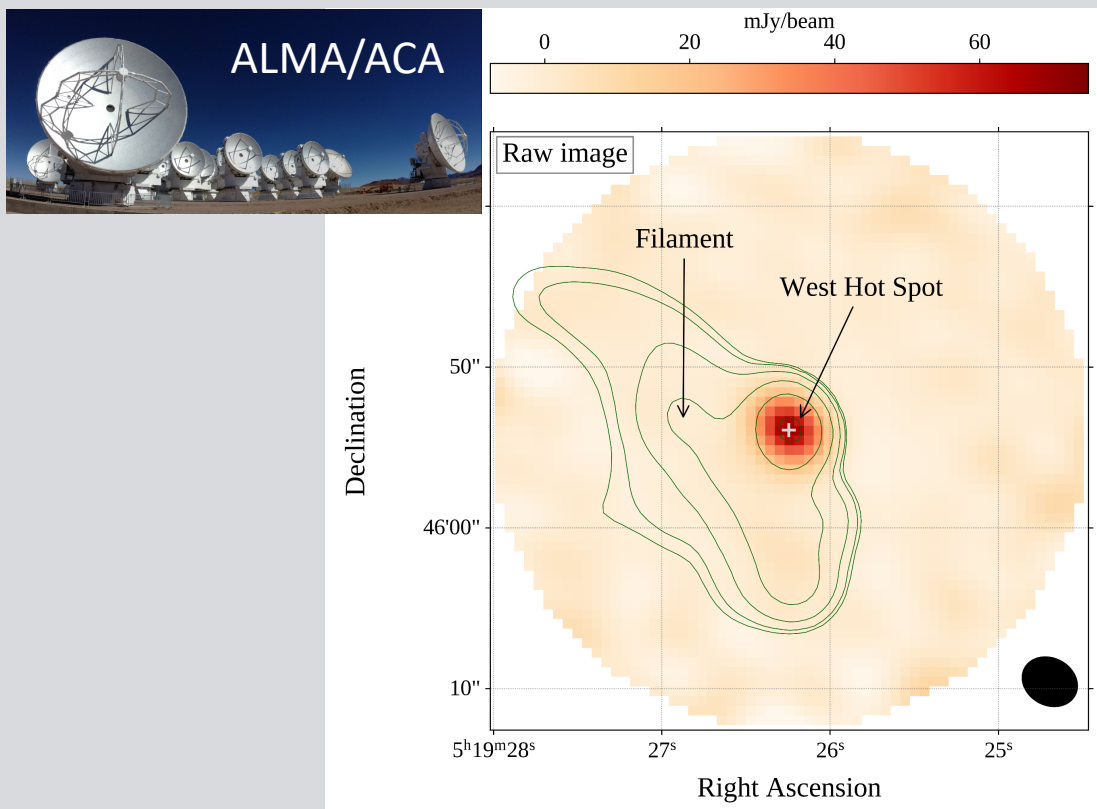
- Far-IR data with Herschel/SPIRE (350 μm)



(Isobe et al. 2020)

ALMA/ACA observation

➤ Sub-mm image with ALMA/ACA

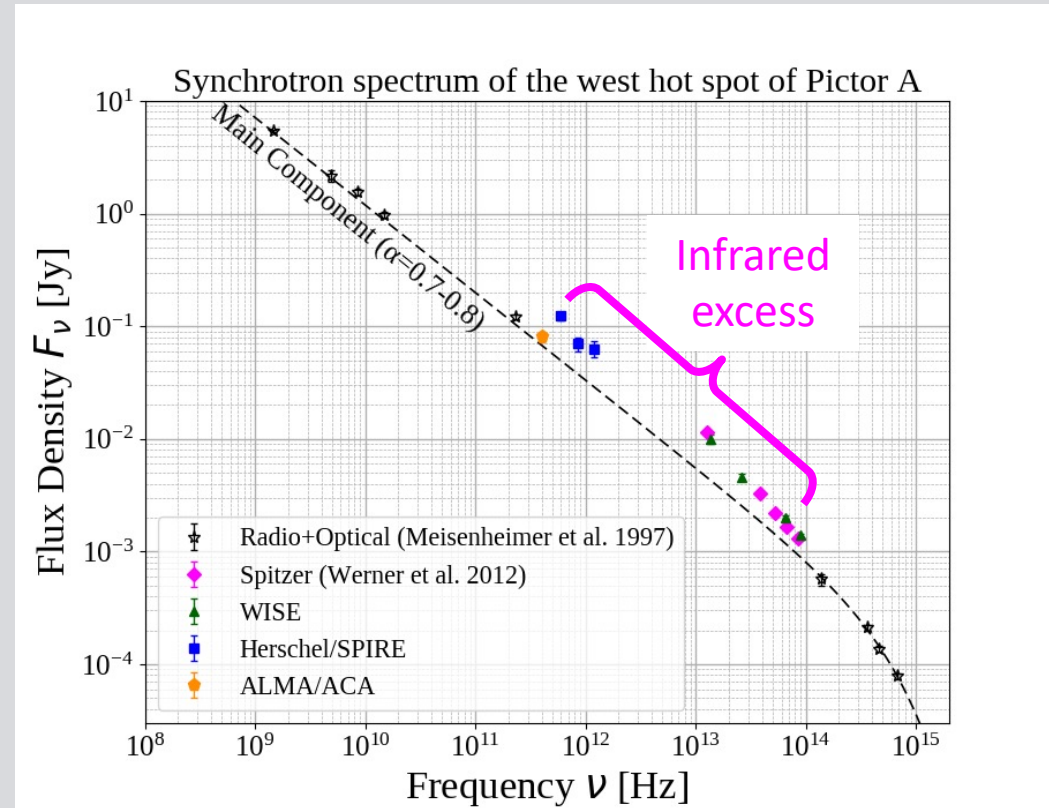
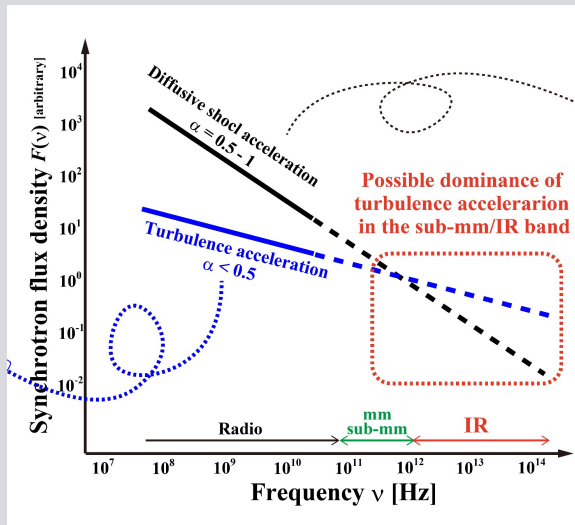


(Isobe et al. 2023)

- ✓ ALMA/ACA observation
 - ✓ Band 8 (405 GHz, 740 μ m)
 - ✓ Beam size: 3.1 arcsec
 - ✓ Conducted on July 26, 2022
- ✓ **A sub-mm source** detected at the position of the west hot spot.
 - ✓ $F_{\nu}(405 \text{ GHz}) = 80.7 \pm 3.1 \text{ mJy}$
- ✓ Positional coincidence
 - ✓ $\sim 75 \text{ mas}$ to the radio peak
 - ✓ $\sim 310 \text{ mas}$ to the WISE source
- ✓ **No sub-mm contaminating source**
 - ✓ Far-infrared emission probably originates in **the west hot spot itself**.

Infrared excess from the west hot spot of Pictor A

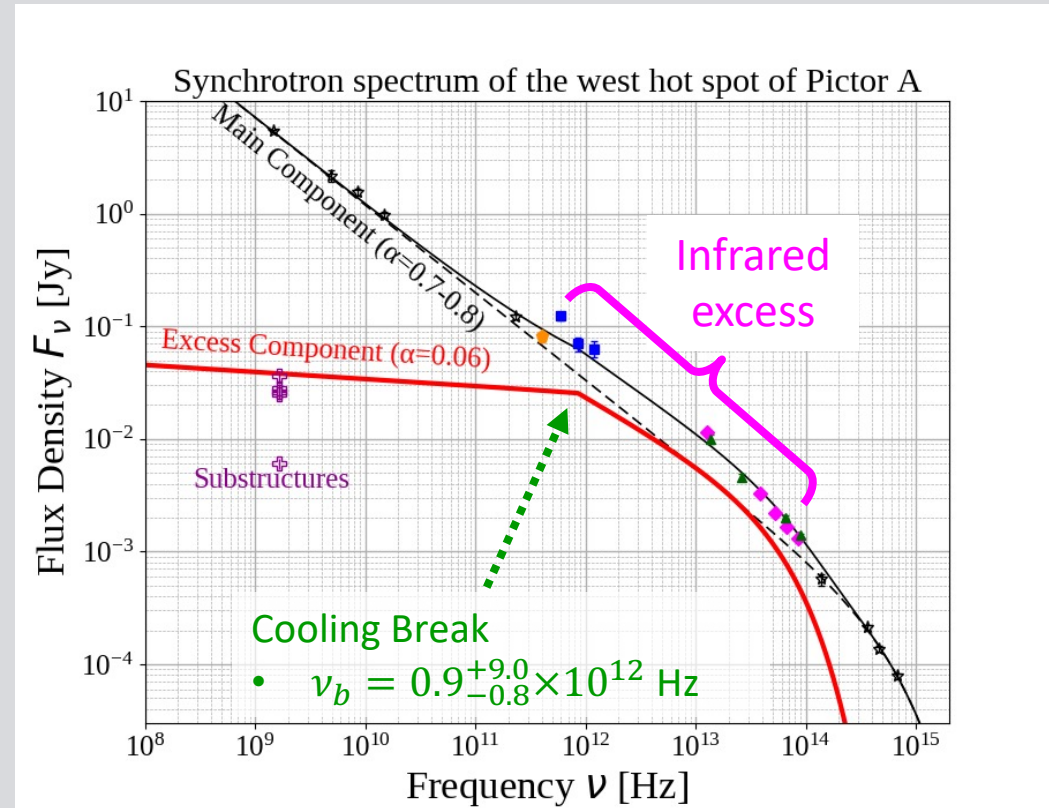
- ✓ The **mid-to-far infrared** data exhibit a **clear excess** over the main synchrotron component.
- ✓ **A deviation from the standard picture.**
- ✓ The sub-mm flux with ALMA/ACA is found to be unaffected by the infrared excess.



(Isobe et al. 2023)

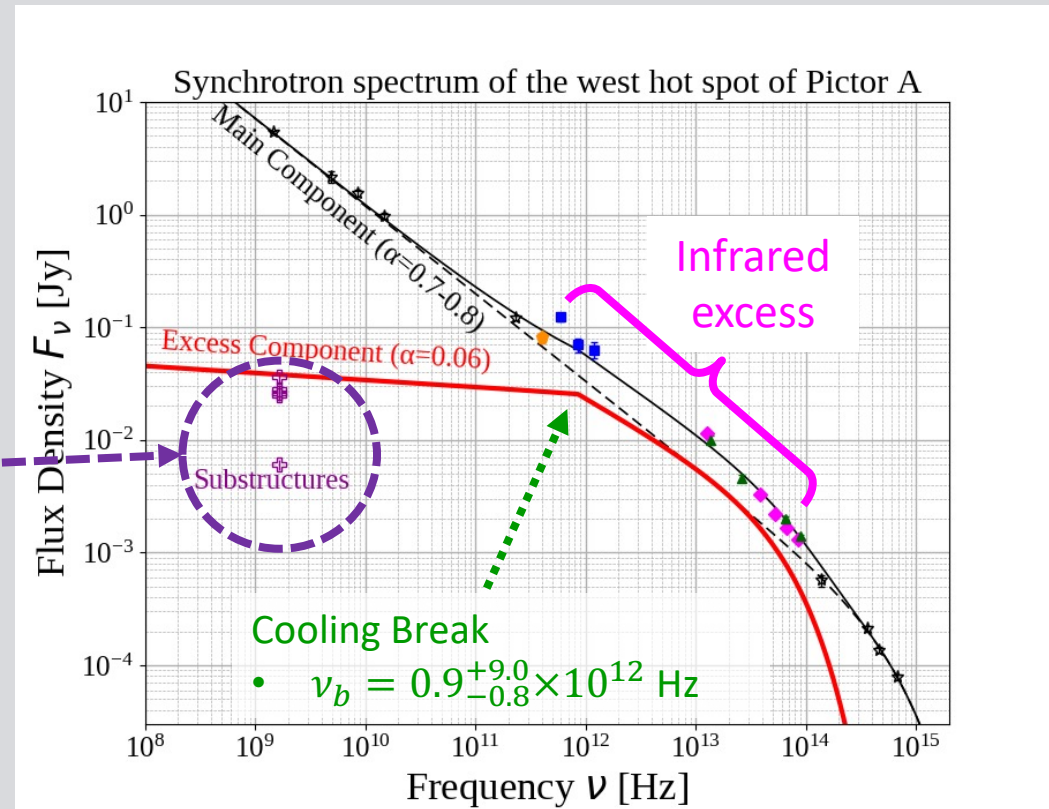
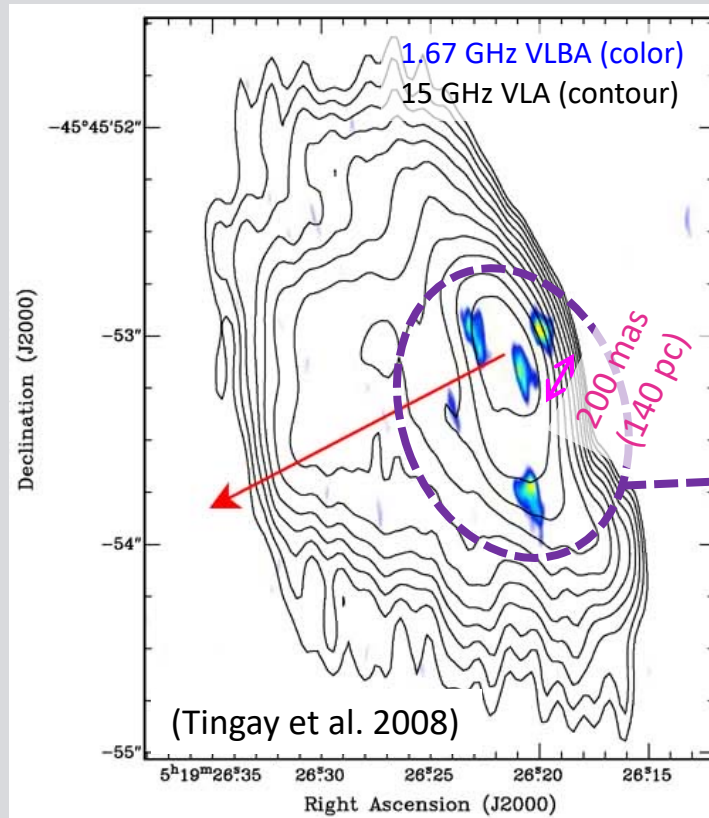
Infrared excess from the west hot spot of Pictor A

- ✓ The **mid-to-far infrared** data exhibit a **clear excess** over the main synchrotron component.
 - ✓ A **deviation from the standard picture**.
 - ✓ The sub-mm flux with ALMA/ACA is found to be unaffected by the infrared excess.
- ✓ The infrared excess is described with a **broken power-law model** subjected to a high-frequency cut off.
 - ✓ $\Delta\alpha = 0.5$ (i.e., cooling break): consistent to **continuous energy injection** accompanied with a **significant radiative cooling**.
- ✓ The low-frequency spectral index of the excess component ($\alpha = 0.06 \pm 0.35$) is **unattributable to the diffusive shock acceleration**.



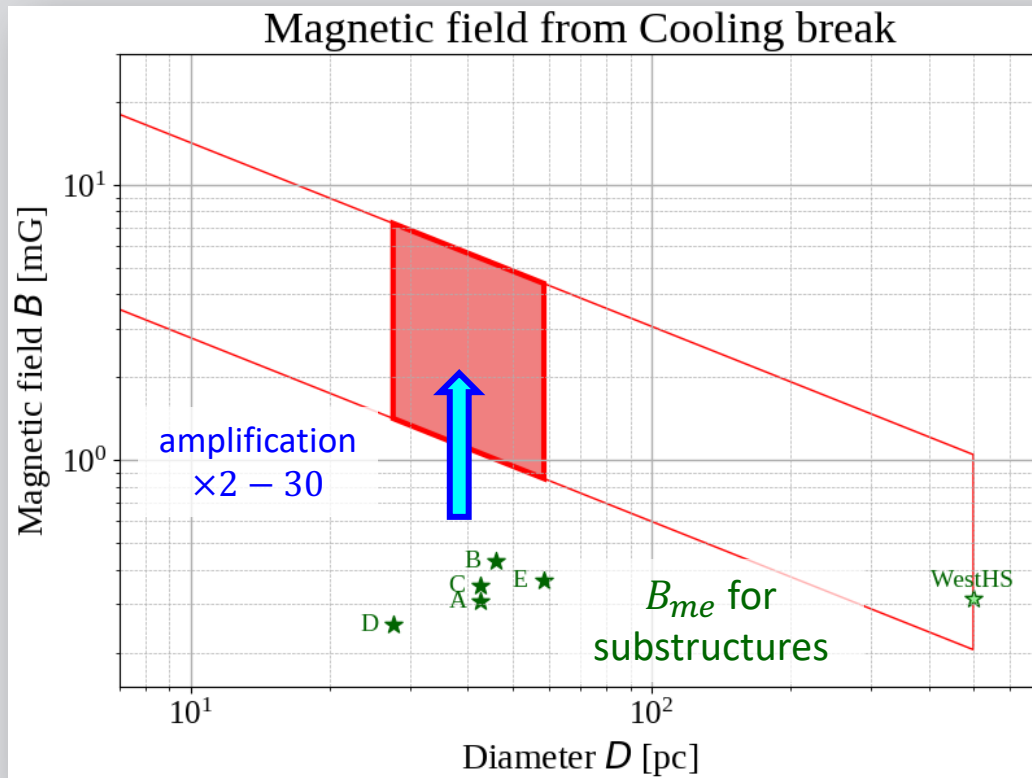
A signature of the **turbulence acceleration**

Substructures as a possible origin of the infrared excess



Substructures as a possible site of the turbulence acceleration

Magnetic field for the infrared excess



✓ Magnetic field estimated from cooling break

✓ $B^3 \simeq \frac{27\pi m_e v^2 c}{\sigma_T^2} D^{-2} v_b^{-1}$ (e.g., Inoue & Takahara 1996)

✓ m_e : electron mass

✓ σ_T : Thomson cross section

✓ v : flow speed

✓ c : speed of light

✓ D : region size

✓ Mutual balance between the radiative cooling and dynamical/adiabatic timescales

✓ Successful application to hot spots (Isobe et al. 2017, 2020, Sunada et al. 2022)

✓ Derived magnetic field: $B = 0.86 - 7.2 \text{ mG}$

✓ $v_b = 0.9_{-0.8}^{+9.0} \times 10^{12} \text{ Hz}$ for the excess component.

✓ A factor of 2 – 30 higher than the minimum-energy magnetic fields (Miley 1980).

✓ $B_{me} = 0.28 - 0.48 \text{ mG}$ for the substructures

✓ Consistent to the magnetic field amplification via the magnetic turbulence (e.g., Inoue et al. 2009, Mizuno et al. 2011).

Summary

- ✓ Hot spots of radio galaxies
 - ✓ Compact regions with a high radio/X-ray flux at the terminal of the AGN jets
 - ✓ Particle acceleration via the diffusive shock acceleration (the standard picture)
- ✓ The **turbulence acceleration** as another important acceleration process in the hot spots.
 - ✓ A possible signature is expected **in the sub-mm to infrared range**, thanks to its spectral hardness.
- ✓ Investigation into the multi-wavelength data of **the west hot spot of Pictor A**.
 - ✓ The radio and optical data alone are consistent to the standard diffusive shock acceleration.
 - ✓ The sub-mm to infrared data with ALMA/ACA, Herschel/SPIRE and WISE data reveals **a significant excess in the infrared range**.
 - ✓ The spectrum of the infrared excess is successfully described with **a broken power-law model**. This spectral shape is consistent to a **particle acceleration** under a **continuous energy injection** accompanied with a **radiative cooling**.
 - ✓ The spectrum of the infrared excess below the break ($\alpha = 0.06 \pm 0.35$) is not ascribed to the standard diffusive shock acceleration ($\alpha > 0.5$). **The hard spectrum of the infrared excess favors a turbulence acceleration.**
 - ✓ The VLBI image reveals **100 pc-scale substructures within the west hot spot**. The substructures are proposed to be an origin of the infrared excess.
 - ✓ By assuming that the substructures are the origin of the infrared excess, the magnetic field strength for the infrared excess is evaluated as **$B = 0.86 - 7.2$ mG** from the break frequency (i.e., the cooling break).
 - ✓ The estimated magnetic field is by a factor of 2 – 30 times higher than the minimum-energy magnetic field. This high magnetic field is consistent to the picture of **the magnetic-field amplification by the turbulence**.

Infrared and sub-mm study of the west hot spot of Pictor A

THE ASTROPHYSICAL JOURNAL, 953:76 (7pp), 2023 August 10
© 2023. The Author(s). Published by the American Astronomical Society.
OPEN ACCESS
<https://doi.org/10.3847/1538-4357/ace04d>
CrossMark

ALMA ACA Detection of Submillimeter Emission Associated with the Western Hot Spot of the Radio Galaxy Pictor A

Naoki Isobe¹, Hiroshi Nagai^{2,3}, Motoki Kino^{2,4}, Shunsuke Baba^{2,5}, Takao Nakagawa¹, Yuji Sunada⁶, and Makoto Tashiro^{1,6}

¹Institute of Space and Astronautical Science (ISAS), Japan Aerospace Exploration Agency (JAXA), 3-1-1 Yoshinodai, Chuo-ku, Sagami-hara, Kanagawa, 252-5210, Japan; n-isobe@ir.isas.jaxa.jp
²National Astronomical Observatory of Japan, 2-21-1 Osawa, Mitaka, Tokyo, 181-8588, Japan
³Department of Astronomical Science, The Graduate University for Advanced Studies, SOKENDAI, 2-21-1 Osawa, Mitaka, Tokyo 181-8588, Japan
⁴Kogakuin University of Technology & Engineering, Academic Support Center, 2665-1 Nakano, Hachioji, Tokyo, 192-0015, Japan
⁵Graduate School of Science and Engineering, Kagoshima University, 1-21-35 Korimoto, Kagoshima, Kagoshima 890-0065, Japan
⁶Department of Physics, Saitama University, 255 Shimo-Okubo, Sakura-ku, Saitama, 338-8570, Japan
Received 2023 March 13; revised 2023 June 14; accepted 2023 June 19; published 2023 August 3

Abstract

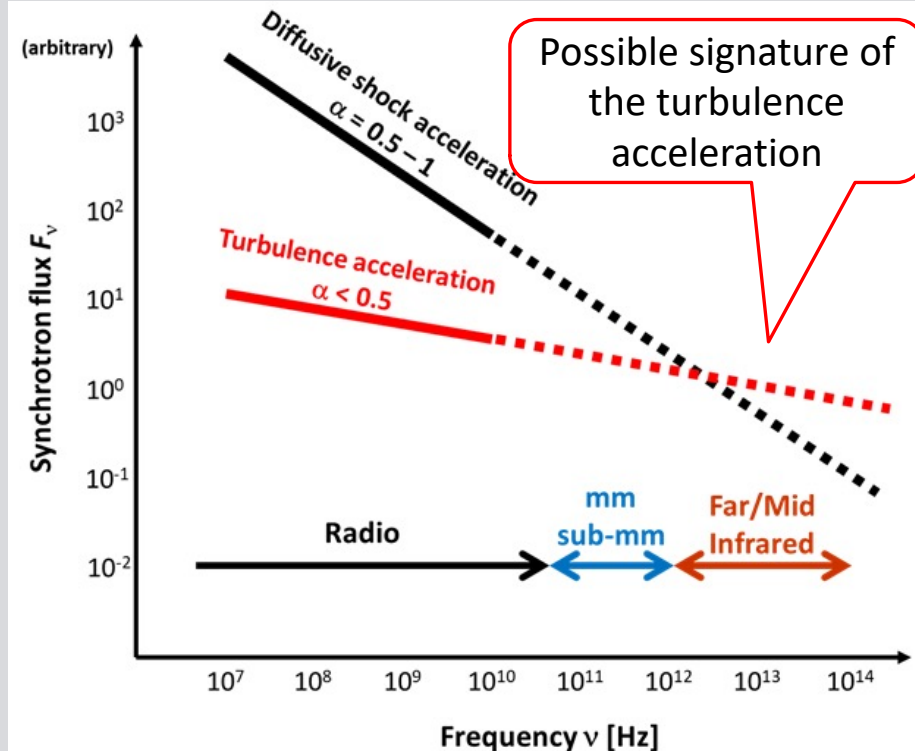
In order to investigate the far-infrared excess detected from the western hot spot of the radio galaxy Pictor A with the Herschel observatory, submillimeter photometry is performed with the Atacama Compact Array (ACA) of the Atacama Large Millimeter/submillimeter Array at Band 8 with the reference frequency of 405 GHz. A submillimeter source is discovered at the radio peak of the hot spot. Because the 405 GHz flux density of the source, 80.7 ± 3.1 mJy, agrees with the extrapolation of the synchrotron radio spectrum, the far-infrared excess is suggested to exhibit no major contribution at the ACA band. In contrast, by subtracting the power-law spectrum tightly constrained by the radio and ACA data, the significance of the excess in the Herschel band is well confirmed. No diffuse submillimeter emission is detected within the ACA field of view, and thus, the excess is ascribed to the western hot spot itself. In comparison to the previous estimate based on the Herschel data, the relative contribution of the far-infrared excess is reduced by a factor of ~ 1.5 . The spectrum of the excess below the far-infrared band is determined to be harder than that of the diffusive shock acceleration. This strengthens the previous interpretation that the excess originates via the magnetic turbulence in the substructures within the hot spot. The ACA data are utilized to evaluate the magnetic field strength of the excess and of diffuse radio structure associated with the hot spot.

Unified Astronomy Thesaurus concepts: Radio hot spots (1344); Relativistic jets (1390); Non-thermal radiation sources (1119); Fanaroff-Riley radio galaxies (526); Magnetic fields (994); Radio interferometers (1345)

- ✓ Isobe et al. 2023, ApJ, 953, 76
- ✓ ALMA ACA Detection of Submillimeter Emission Associated with the Western Hot Spot of the Radio Galaxy Pictor A
- ✓ Isobe et al. 2020, ApJ, 899, 17
- ✓ Herschel SPIRE Discovery of **Far-infrared Excess** Synchrotron Emission from the West Hot Spot of the Radio Galaxy Pictor A
- ✓ Isobe et al. 2017, ApJ, 850, 193
- ✓ **Mid-infrared Excess** from the West Hot Spot of the Radio Galaxy Pictor A Unveiled by WISE

Spectrum of the turbulence acceleration

➤ Comparison between the diffusive shock and turbulence accelerations



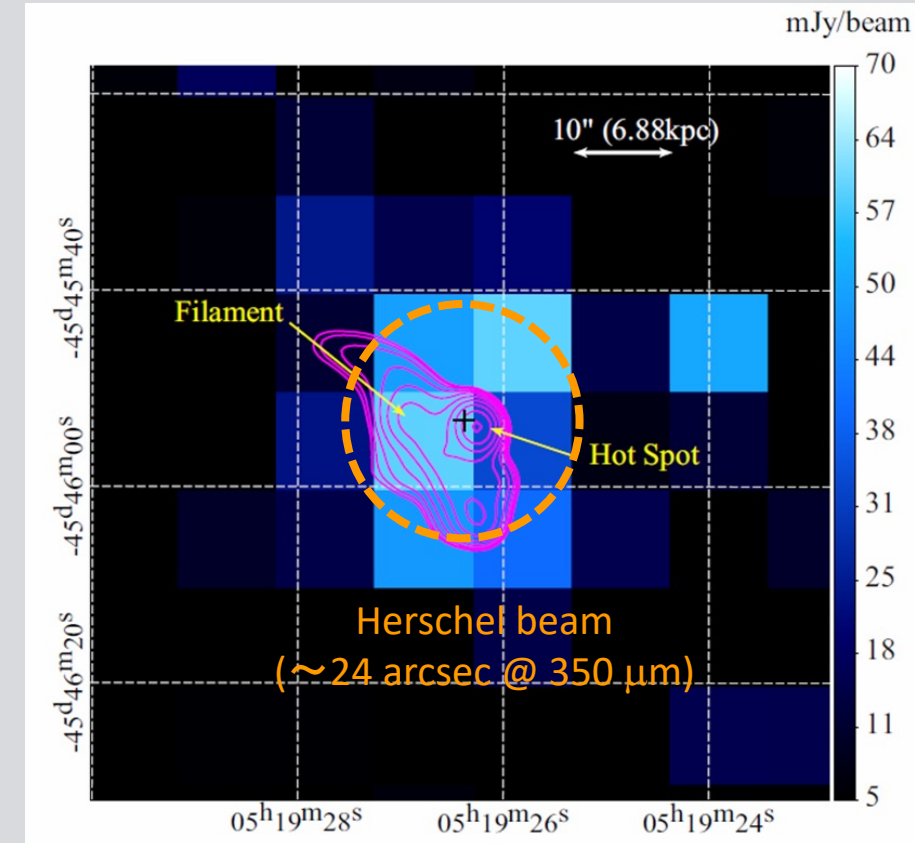
- ✓ Spatial spectrum of the magnetic turbulence
 - ✓ $|\delta B^2|_k \propto k^{-q} \ (1 < q < 2)$
 - ✓ k : spatial wavenumber of the turbulence
- ✓ Spectrum of the accelerated electrons
 - ✓ Number density: $N(\varepsilon_e) \propto \varepsilon_e^{-p} \propto \gamma^{-p}$
 - ✓ Spectral index: $p = q - 1$
- ✓ Synchrotron spectrum
 - ✓ Flux density: $F_\nu \propto \nu^{-\alpha}$
 - ✓ Spectral index: $\alpha = \frac{p-1}{2}$

Spectral index	Turbulence		Strong shock
	Kolmogorov	Hard sphere	
Turbulence q	5/3	2	–
Electrons p	2/3	1	2
Synchrotron α	–1/6	0	0.5

Importance of ALMA/ACA observations

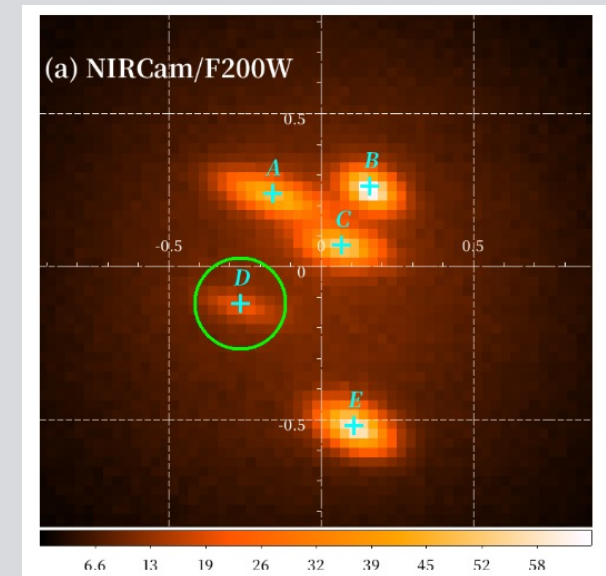
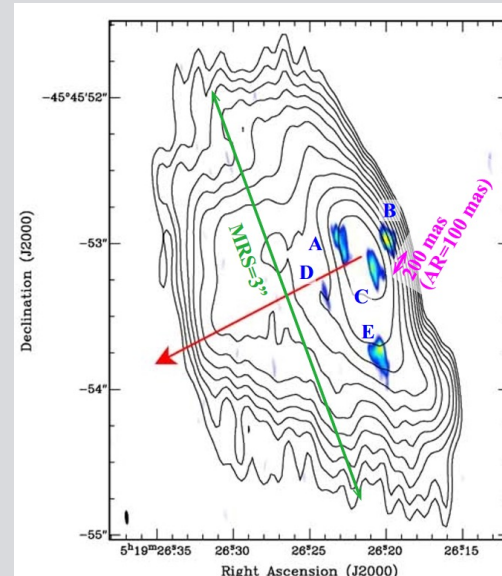
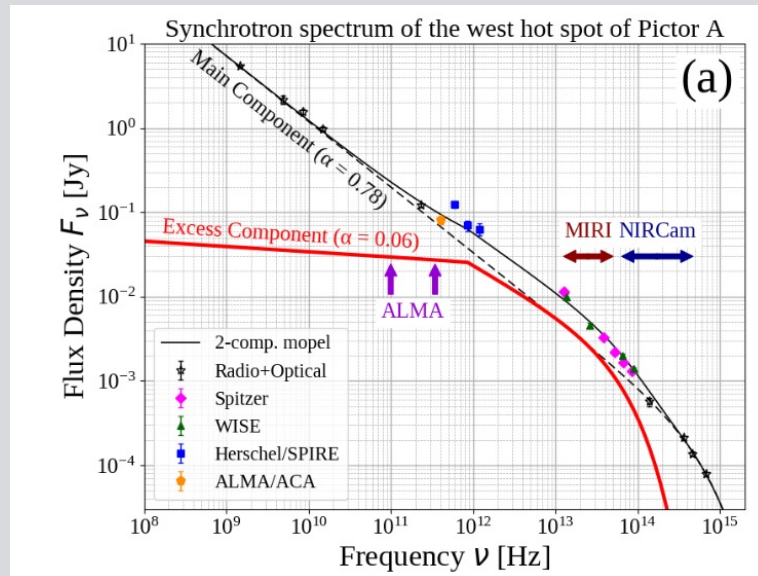
- ✓ The large Herschel/SPIRE beam
 - ✓ 23.9 arcsec @ 350 μm (856 GHz)
 - ✓ 16.7 arcsec @ 250 μm (1.2 THz)
- ✓ A possible contamination from the diffuse structure (e.g., filament) to the Herschel/SPIRE data should be removed
- ✓ ALMA/ACA at Band 8 is the ideal tool

Parameter	Requirements	ACA Band 8
Frequency	Quasi-overlap with Herschel	405 GHz (740 μm)
Beam size	A few arcsec	3.1 arcsec
MRS	> 10 arcsec	16.6 arcsec



Future studies with ALMA and JWST

➤ Direct sub-mm/infrared imaging of the substructures for direct evidence



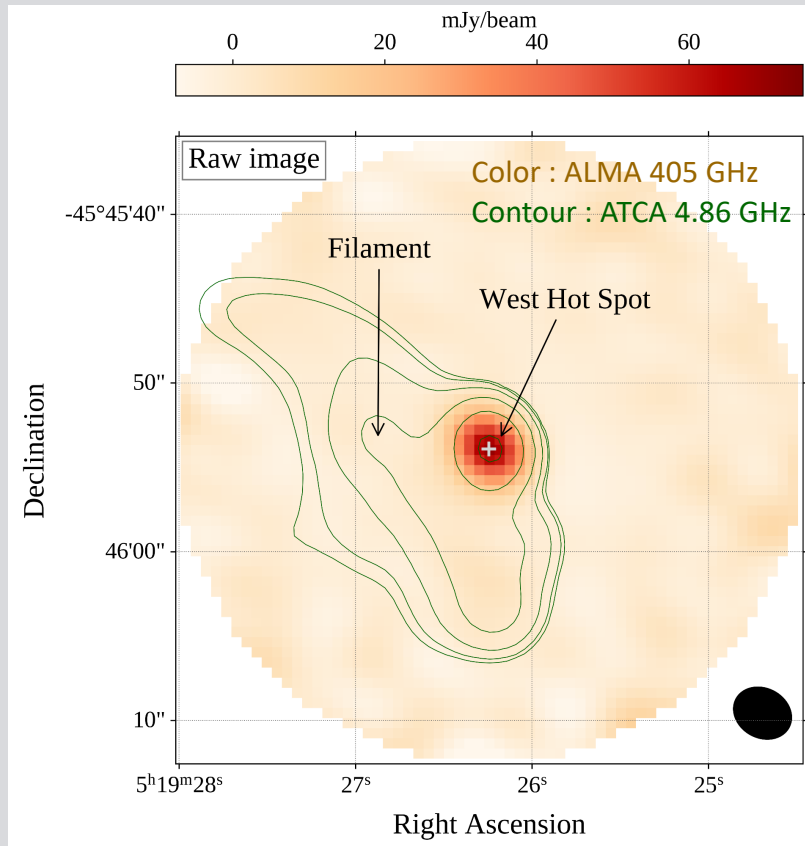
- Requirements
 - Beam size: $\Delta\theta=100$ mas
 - Max. recoverable size: 3 arcsec
 - (Polarimetry)

ALMA Capability
C3 + C6 configuration at Band 8
C5 + C8 configuration at Band 6

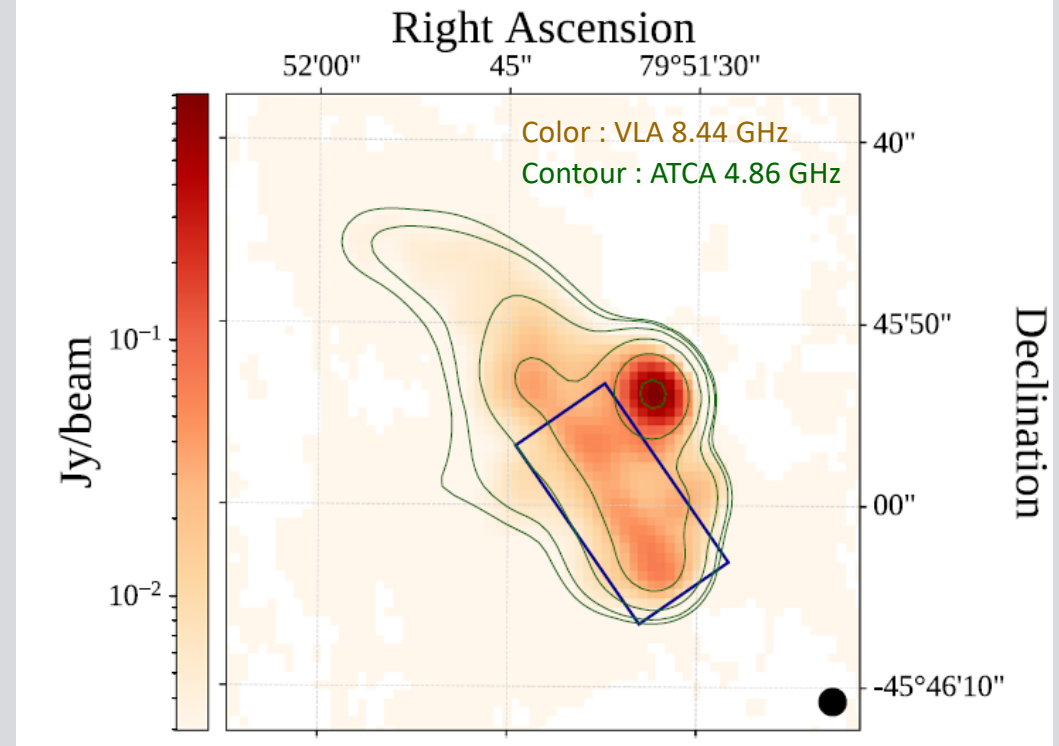
JWST capability
Simulated JWST NIRCams
image at $\lambda = 2$ mm

Filament associated to the west hot spot

➤ Sub-mm image with ALMA/ACA



➤ GHz radio image

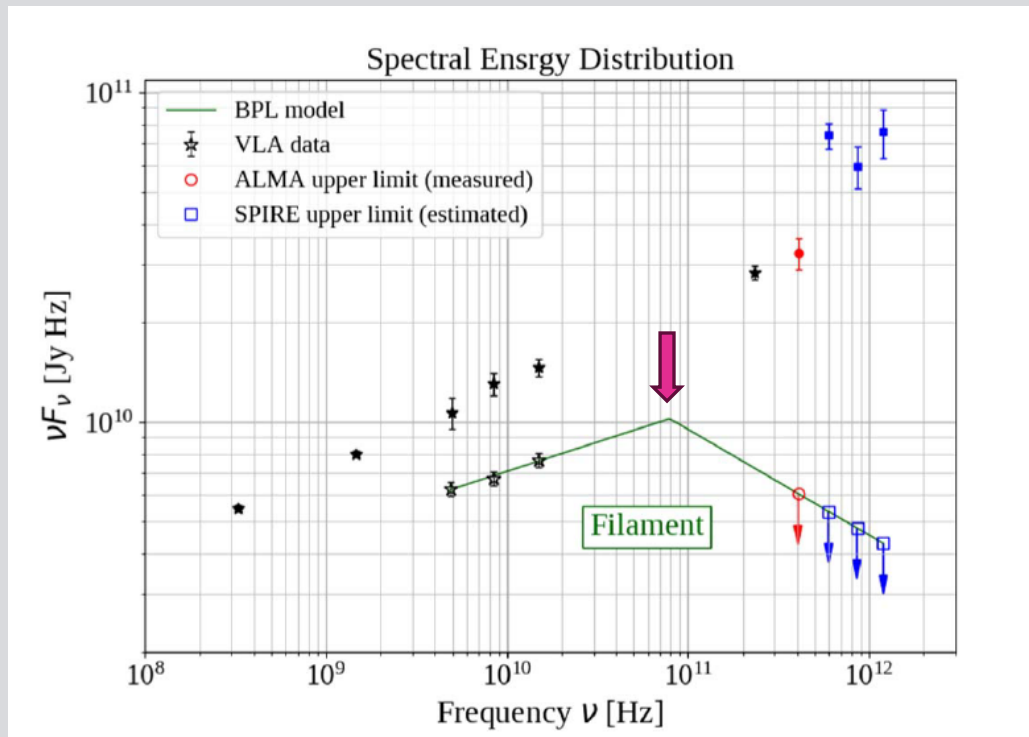


Filament

- Back/lateral-flow plasma leaked from the hot spot (Saxton et al. 2002; Mizuta et al. 2010).

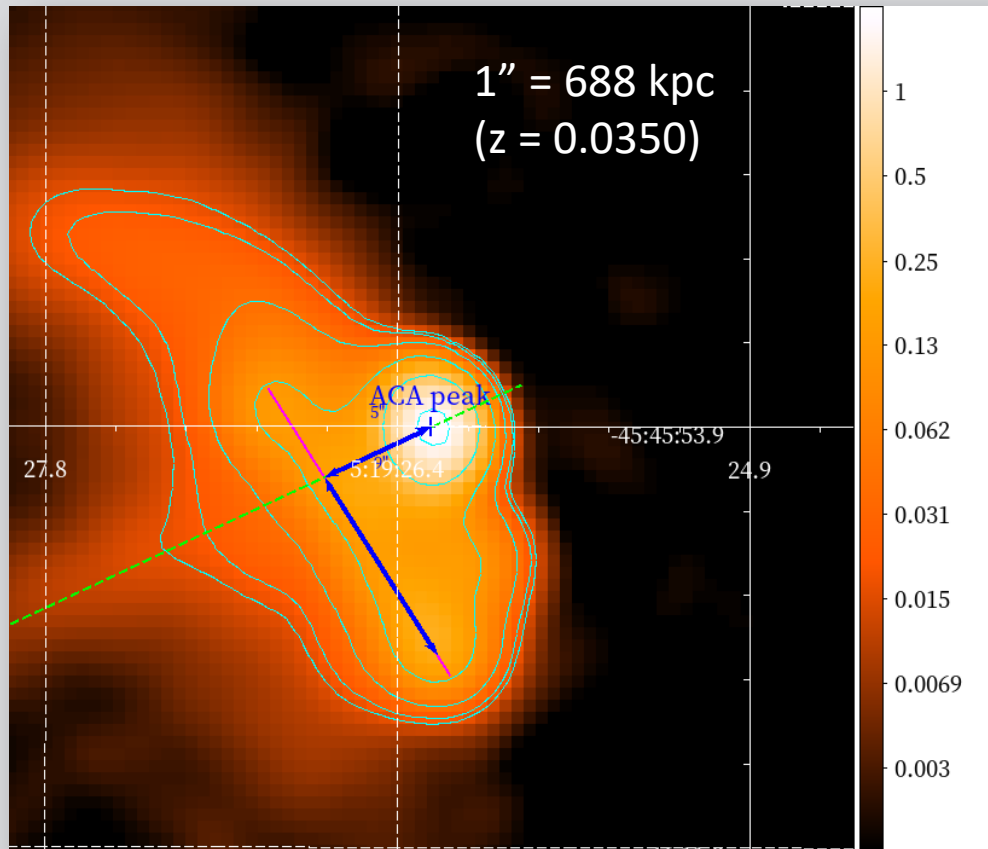
Cooling break of the filament

➤ Synchrotron spectrum of the filament



- ✓ Synchrotron spectrum in the GHz range
- ✓ Synchrotron flux is significantly detected
 - ✓ $F_\nu(8.44 \text{ GHz}) = 0.80 \pm 0.04 \text{ Jy}$
- ✓ The spectrum of the filament is consistent to the picture of the back/lateral flow plasma
 - ✓ $\alpha = 0.82 \pm 0.06$
 - ✓ Agree with the index of the west hot spot
- ✓ Constraint on the **cooling break**
 - ✓ Upper limit on the ALMA flux
 - ✓ $F_\nu(405 \text{ GHz}) < 15 \text{ mJy}$
 - ✓ $\nu_b < 8 \times 10^{10} \text{ Hz}$

Magnetic field of the filament



✓ Magnetic field estimated from the cooling break

$$B^3 \simeq \frac{27\pi e m_e v^2 c}{\sigma_T^2} D^{-2} v_b^{-1}$$

✓ Region size

✓ Case 1 (back flow case): $D = 5'' = 3.44$ kpc

✓ Distance from the hot spot along the jet

✓ Case 2 (lateral flow): $D = 9'' = 6.19$ kpc

✓ Distance from the hot spot orthogonal to the jet

✓ Constraint on the magnetic field:

✓ Case 1: $B > 280$ mG

✓ Case 2: $B > 190$ mG

✓ Cooling break for the filament: $\nu_b < 8 \times 10^{10}$ Hz

✓ Minimum-energy magnetic field of the filament

✓ $B_{me} \sim 30$ mG

✓ Possible magnetic-field amplification via the turbulence

✓ $B/B_{me} = 5 - 10$